Nuclear moments of ^{179}Ta from optical measurement of hyperfine structure

M. Wakasugi,[1] W. G. Jin,[1] M. G. Hies,[1] T. T. Inamura,[2] T. Murayama,[3] T. Ariga,[4] T. Ishizuka,[4] T. Wakui,[5] H. Katsuragawa,[5] J. Z. Ruan,[6] I. Sugai,[7] and A. Ikeda[8]

[1]*Cyclotron Laboratory, The Institute of Physical and Chemical Research (RIKEN), Wako-shi, Saitama 351-01, Japan*
[2]*Safety Center, The Institute of Physical and Chemical Research (RIKEN), Wako-shi, Saitama 351-01, Japan*
[3]*Department of Physics, Tokyo University of Mercantile Marine, Koto-ku, Tokyo 135, Japan*
[4]*Department of Physics, Saitama University, Urawa-shi, Saitama 338, Japan*
[5]*Department of Physics, Toho University, Funabashi-shi, Chiba 274, Japan*
[6]*Department of Physics, Rikkyo University, Toshima-ku, Tokyo 171, Japan*
[7]*Institute of Nuclear Physics, University of Tokyo, Tanashi-shi, Tokyo 188, Japan*
[8]*Sizuoka Institute of Science and Technology, Fukuroi-shi, Shizuoka 437, Japan*

We have made high-resolution laser spectroscopy of the hyperfine structure of a radioactive isotope ^{179}Ta ($T_{1/2}=1.8$ y) using an argon-ion sputtering atomic-beam source. From hyperfine constants A and B of the atomic ground state ($^4F_{3/2}\ 5d^36s^2$), the magnetic dipole and electric quadrupole moments of the nuclear ground state of ^{179}Ta ($I=7/2$) have been determined for the first time: $\mu_I^{179}=2.289(9)\ \mu_N$ and $Q_s^{179}=3.37(4)$ b. It is pointed out that magnetic moments of the ground and isomeric states in the region $N=102-112$ can be systematically described in terms of the presently available theory while the revealed systematic behavior of electric quadrupole moments is hardly reproduced by the theory.

I. INTRODUCTION

Measurements of hyperfine structures and isotope shifts by means of laser spectroscopy have been extensively made to derive the nuclear electromagnetic moments and changes of nuclear charge radii [1]. These studies have been very fruitful in the understanding of nuclear structure. However, only few reports [2–5] of laser spectroscopy of radioactive isotopes in the region of refractory elements ($Z=72-77$) have been published because there has been no powerful and versatile tool to produce intense and stable ion beams or atomic beams of the refractory element.

Isotopes in this region are very interesting from the nuclear-structure viewpoint since they are in a well-deformed region, possessing a number of high-spin isomers. A radioactive isotope ^{179}Ta ($T_{1/2}=1.8$ y) for instance has been investigated about the yrast level scheme and the rotational band structure by means of in-beam spectroscopy using reactions such as (p,n) and $(d,2n)$ [6], (^{7}Li,$4n$) [7], and (p,t) [8]; many high-spin isomeric states, which arise from high-K multiquasiparticle states, have also been discovered, but there are no data available on the static electromagnetic properties of the nucleus.

We have developed a powerful and versatile source of atomic beams using the argon-ion sputtering method to make high-resolution laser spectroscopy of hyperfine structures and isotope shifts for refractory elements [9]. With this system, we started a systematic laser spectroscopy of Ta and Hf isotopes. First, we determined the electric quadrupole moment of ^{180m}Ta, which is a naturally occurring radioactive isotope with an extremely long lifetime ($T_{1/2}>10^{15}$ y) and high-spin $I=9^-$, by means of a laser-rf double-resonance technique [10]. In the present work we shall report the first determination of electromagnetic moments of the nuclear ground state of the radioactive isotope ^{179}Ta from the hyper-

fine structure. The present result being combined with our previous data on ^{180m}Ta has led to a systematic review of nuclear moments in the region $N=102-112$.

II. EXPERIMENT

A. Laser spectroscopy system

The experimental setup, which is an off-line laser spectroscopy system, is schematically shown in Fig. 1. Metallic samples with a typical size of 8 mm×15 mm were placed on a sample holder that can be moved in three dimensions with stepping motors. The sample atoms were sputtered by 10-keV argon ions. Sputtered atoms were collimated by three
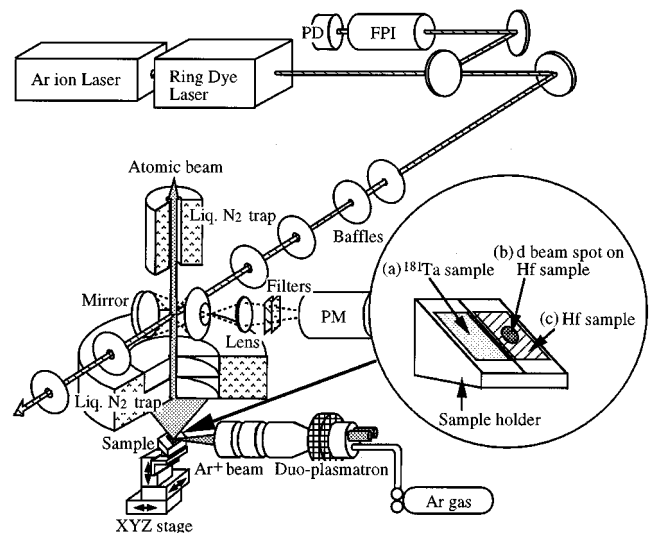

FIG. 1. Experimental setup. Details of the sample set on the sample holder are shown in the inset.

diaphragms with an aperture of 4 mm in diameter; the intensity of the collimated atomic beam was about 10^{10} atoms per s at an argon-ion beam current of 0.5 mA. The size of the argon-ion beam spot on the sample was about 1 mm in diameter.

A laser beam from a ring dye laser (Coherent 699-29) pumped with an argon-ion laser (Spectra Physics 171) was guided into a vacuum chamber and crossed with the atomic beam perpendicularly to avoid Doppler broadening. Fluorescence photons from the crossing point were collected and focused on a cooled photomultiplier (Hamamatsu 1333) using spherical mirrors and a lens. Transmitted light signals of a confocal Fabry-Perot interferometer with a free spectral range of 149.77(3) MHz were recorded simultaneously with the fluorescence signals. This system enables us to measure the fluorescence spectrum of Ta atoms with an abundance of 10 ppm in the sample. Details of this system were described in our previous papers [9,11].

B. Preparation of radioactive ^{179}Ta sample

We prepared a sample of radioactive ^{179}Ta atoms by bombarding a 97% natural Hf target (0.25-mm thick) with a 19-MeV deuteron beam from the RIKEN AVF cyclotron. Reactions of ^{180}Hf$(d,3n)$ and ^{179}Hf$(d,2n)$ used were expected to have cross sections of about 1.2 and 0.6 b at d energies of 19 and 12 MeV, respectively, by the ALICE code [12]. The total current of the d beam was 0.6 C. The size of the d-beam spot on the Hf target was about 6 mm^2. Most of ^{179}Ta atoms were mainly located at the depth less than 0.1 mm from the surface. Since ^{179}Ta decays without emitting gamma rays, we estimated the number of produced ^{179}Ta atoms from measurement of the gamma rays coming from the decay of ^{177}Ta ($T_{1/2}$=2.36 d), which was simultaneously produced by ^{178}Hf$(d,3n)$ and ^{177}Hf$(d,2n)$ reactions. The number of ^{179}Ta atoms was thus estimated to be 5×10^{14} atoms, which were produced in a small volume of 0.6 mm^3 in the Hf target, i.e., the abundance of ^{179}Ta in the volume was about 20 ppm.

After cooling off short-lived isotopes such as ^{177}Ta, we set the radioactive sample on the sample holder in the off-line laser spectroscopy system. A natural Ta sample for reference was also set together with the radioactive one as shown in the inset of Fig. 1.

C. Measurement of hyperfine structure of ^{179}Ta

The hyperfine structure of ^{179}Ta should be similar to that of ^{181}Ta because ^{179}Ta has the same nuclear spin as ^{181}Ta. We first observed an optical hyperfine spectrum of a 540.3-nm transition from the ground state $^4F_{3/2}$ to a 18 504.7 cm^{-1} $^4D_{1/2}$ level of the stable isotope ^{181}Ta to check wavelengths of the laser, geometrical conditions of the mirror and sample position, and focusing of the argon-ion beam on the sample; these conditions were optimized to get as much fluorescence signals as possible. The hyperfine spectrum observed for ^{181}Ta is shown in Fig. 2(a). There are six hyperfine peaks labeled by alphabets $a-f$ which correspond to the hyperfine transitions shown in Fig. 3. Next, we moved the sample so that the argon-ion beam struck the center of the d-beam spot on the radioactive sample (see the inset of Fig. 1). At this position, we measured the fluorescence spectrum three times at the same wavelength region as in Fig. 2(a). We took a
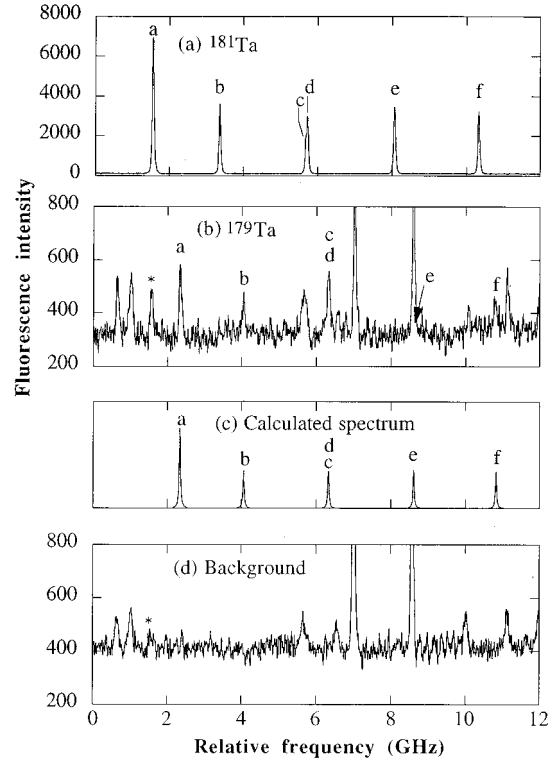

FIG. 2. Measured spectra of the 540.3-nm transition in radioactive ^{179}Ta with reference spectra: The spectrum (a) was obtained when the natural Ta sample was bombarded with a 10-keV argon-ion beam as shown in Fig. 1; during the same bombardment the spectrum (b) was obtained for the center of the d-beam spot on the radioactive sample, and the spectrum (c) shows the hyperfine spectrum reproduced using hyperfine constants obtained here (see Table II) for ^{179}Ta; the background spectrum (d) for a point outside the d-beam spot on the radioactive sample.

summation of observed three spectra, which is shown in Fig. 2(b). In this spectrum 14 resonance peaks were observed with significant yields. To identify them, we measured a background spectrum by bombarding a point outside of the d-beam spot on the radioactive sample with the argon-ion beam [see the inset of Figs. 1 and 2(d)]. We identified the four peaks labeled a, b, $c(d)$, and f in Fig. 2(b) which are not coming from the background.
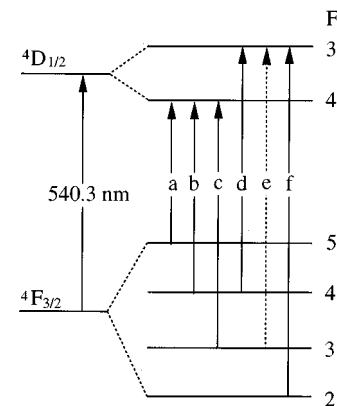

FIG. 3. Hyperfine transitions of ^{179}Ta. Transitions labeled $a-f$ correspond to peaks marked with a–f in the spectrum of Fig. 2.

TABLE I. Experimental hfs line separation in ^{179}Ta together with that in ^{181}Ta for comparison.

Transition	Separation (MHz)	
	^{179}Ta	^{181}Ta
a-b	1712 (4)	1822.4 (4)
a-c	3999(20)[a]	4147.9(10)
a-d	3999(20)[a]	4197.0(10)
a-e		6522.5(16)
a-f	8473 (7)	8722.8(22)

[a]The errors quoted are coming from the FWHM of the peak $c(d)$ because the c and d transitions energetically coincide with each other.

A peak asterisked in Figs. 2(b) and (d) was found to be the strongest component of hyperfine transitions in ^{181}Ta. The reason why this peak of ^{181}Ta was observed is that a small amount of ^{181}Ta atoms sputtered from the natural Ta sample adhered to the surface of the radioactive sample during the measurement for optimization mentioned above. Atoms of ^{181}Ta on the surface must quickly disappear because of argon-ion sputtering. In fact, this peak disappeared in the second scan onwards at the same position of the argon-ion beam spot on the sample. The other nine peaks with no label in Fig. 2(b) come from impurity atoms or molecules sputtered from the Hf sample. It should also be stated that these background peaks were observed for another Hf sample that was purchased simultaneously without d-beam bombardment.

The hyperfine peaks of ^{179}Ta have been identified as labeled by alphabets a–f in the following procedure. The experimental line separations obtained in Fig. 2(b) are presented in Table I. Here Zeeman splittings of the hyperfine levels due to a stray magnetic field are negligibly small compared with the experimental linewidth. Assuming that these lines a, b, $c(d)$, and f correspond to the transitions a, b, $c(d)$, and f between the hyperfine levels as shown in Fig. 3 like the case of ^{181}Ta, we made a least-squares fit to the experimental line separations with a well-known formula for the hyperfine splitting [13]. Hyperfine constants A and B of the ground state $^4F_{3/2}$ and the excited state $^4D_{1/2}$ thus obtained are summarized in Table II; the previously known values of A and B for ^{181}Ta are given for comparison. Using the A and B constants derived, the hyperfine spectrum of ^{179}Ta is well reproduced as shown in Fig. 2(c); the calculated spectral lines c and d coincide with each other, and the yield of the observed peak at position of c and d is well repro-

duced in the calculation. (The calculation was made using a linewidth of 50 MHz.) The hyperfine transition e, which is indicated by a dotted arrow in Fig. 3, was found accidentally masked by a background peak.

III. NUCLEAR MOMENTS OF ^{179}Ta

We use the hyperfine constants of the ground state $^4F_{3/2}$ to derive the nuclear moments because both the A and B constants for the reference atom ^{181}Ta have been precisely measured by means of laser-rf double-resonance spectroscopy [11]. From the well-established relation of A constants and nuclear magnetic moments between two isotopes [13]

$$\frac{A^{179}}{A^{181}} = \frac{\mu_I^{179}/I^{179}}{\mu_I^{181}/I^{181}}, \tag{1}$$

the magnetic moment μ_I^{179} of ^{179}Ta is derived to be

$$\mu_I^{179} = +2.289(9)\,\mu_N, \tag{2}$$

where the nuclear spin $I^{179}=7/2$, $I^{181}=7/2$, μ_N is the nuclear magneton; and values of A^{181} [11] and μ_I^{181} [14] used are presented in Table II. The error quoted for μ_N^{179} contains an experimental error and the uncertainty of magnetic hyperfine anomaly (Bohr-Weisskopf effect) [15], which is taken into account in the same way as described in our previous paper [10].

The ratio of B constants of two isotopes should also be equal to the ratio of the nuclear spectroscopic quadrupole moments [13],

$$\frac{B^{179}}{B^{181}} = \frac{Q_s^{179}}{Q_s^{181}}. \tag{3}$$

The moment Q_s^{179} of ^{179}Ta is thus derived using the B^{179} constant determined here and known values of B^{181} [11] and Q_s^{181} of ^{181}Ta that is the value estimated from the weighted average of quadrupole moments Q_s compiled in [14] (see Table II):

$$Q_s^{179} = +3.37(4)\ \text{b}. \tag{4}$$

IV. DISCUSSION

It is known that the Nilsson orbital for an unpaired proton in the ground states of Ta isotopes is $7/2^+[404]_\pi$ in the region $N=102$–112 and these isotopes have an isomeric state with another orbital of $9/2^-[514]_\pi$ at a low excitation energy.

TABLE II. Hyperfine constants and nuclear moments of ^{179}Ta together with those of ^{181}Ta for comparison.

	Hyperfine constants			Nuclear moments			
	Ground $^4F_{3/2}$		Excited $^4D_{1/2}$				
Isotope	A (MHz)	B (MHz)	A (MHz)	$\mu_I(\mu_N)$	Q_s (b)	$Q_0{}^a$ (b)	β
^{179}Ta	492(1)	$-1\,043$ (10)	$-569(1)$	$+2.289(9)$	$+3.37(4)$	$+7.22(9)$	0.286(4)
^{181}Ta	509.081 03(9)[b]	$-1\,012.228\,2$ (6)[b]	$-593.65(2)$	$+2.237\,05(7)$[c]	$+3.266(13)$[d]	$+7.00(3)$	0.275(1)

[a]Estimated values from Q_s in the limit of a well-deformed rigid rotor.
[b]Reference [11].
[c]Reference [14].
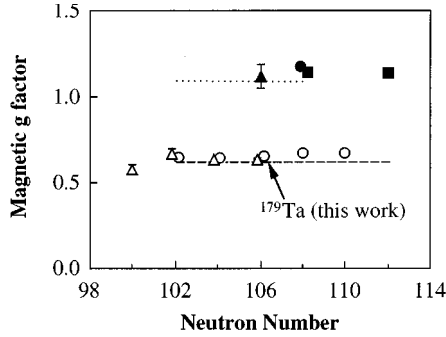[d]Weighted average of experimentally determined values compiled in Ref. [14].

FIG. 4. Systematic trend of the magnetic moments of Ta and neighboring odd-Z elements Lu and Re. Open symbols are for the ground states with the $7/2^+[404]_\pi$ proton orbital, and closed ones for the isomeric states with the $9/2^-[514]_\pi$ proton orbital: circles are for Ta [10,14] including the present data, triangles for Lu [14], and squares for Re [14]. Dashed and dotted lines are theoretical values [16] for the $7/2^+[404]_\pi$ and the $9/2^-[514]_\pi$ states, respectively.

They are normal-parity orbitals and have the highest value of Ω in the major shell they belong to. Since no state in the neighborhood interacts with them through a Nilsson field, they keep having j as a good quantum number: $7/2^+[404]_\pi$ and $9/2^-[514]_\pi$ are well represented by $g_{7/2,7/2}$ and $h_{9/2,9/2}$, respectively. Figure 4 shows magnetic g_I factors $[g_I = \mu_I/(I\mu_N)]$ for states having these proton orbitals in Ta and neighboring odd-Z elements Lu and Re. As is seen from this figure, the missing data on ^{179}Ta is nicely fulfilled in a systematical manner by the present measurement. The g_I factors of the states with the $9/2^-[514]_\pi$ orbital are about two times larger than those of the states with the $7/2^+[404]_\pi$ orbital. Since an unpaired particle mainly contributes to the nuclear magnetic moments, those of states with the same proton orbital should be similar to each other, being independent of elements. In microscopic calculation using single-particle Nilsson wave functions, $g_I = 0.629$ of the ground state with the $7/2^+[404]_\pi$ orbital and $g_I = 1.09$ of the isomeric state with the $9/2^-[514]_\pi$ orbital have been predicted for odd-A Ta isotopes [16]; these values are in good agreement with the experimental ones including the present measurement (see Fig. 4).

We estimate the intrinsic quadrupole moment Q_0 using the spectroscopic quadrupole moment Q_s and a well-known formula based on the strong-coupling limit [17]

$$Q_s = \frac{3K^2 - I(I+1)}{(I+1)(2I+3)} Q_0,\qquad(5)$$

where $K = I$; thus we have $Q_0^{179} = 7.22(9)$ b. This value is slightly larger than that for the ground state of ^{181}Ta.

The intrinsic quadrupole moments known for the ground states with the $7/2^+[404]_\pi$ orbital and the isomeric states with the $9/2^-[514]_\pi$ orbital in Ta isotopes are plotted in Fig. 5. Those for the ground states of Hf isotopes [14,18], which are the core nuclei of Ta isotopes, are also plotted in the figure. There have been only five data reported for Ta isotopes: the ground and isomeric states of ^{181}Ta [14], the ground state of ^{175}Ta [14], and two isomeric states of ^{178m}Ta [14] and ^{180m}Ta [10]. Systematic behavior of the quadrupole moments of both states has become clear by adding data on
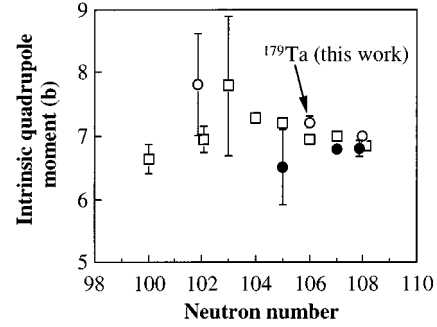

FIG. 5. Systematic trend of the intrinsic quadrupole moments of Ta isotopes and core nuclei Hf. Open circles are for the ground states with the $7/2^+[404]_\pi$ proton orbital in Ta [14] including the present data, closed ones for the isomeric states with the $9/2^-[514]_\pi$ proton orbital [10,14], and squares for the ground states of Hf isotopes [14,18].

^{180m}Ta and ^{179}Ta. The quadrupole moments of the ground states are slightly larger than those of the core-nuclei Hf; by contrast those of isomeric states are just the opposite. The deviations of the moments for both states from the core-nuclei Hf are plotted in Fig. 6; they have opposite signs and it seems that they decrease with increasing neutron number. Theoretical values estimated using single-particle Nilsson wave functions by Ekström *et al.* [16] are shown by $+$ symbols in the figure: their calculation gives the same values for both the ground and isomeric states and cannot represent the behavior revealed experimentally.

We have estimated the change of the quadrupole moment due to adding a proton to the Hf core using an equation which is based on BCS theory:

$$Q_0 = Q_0^c + 2(u_i^2 - v_i^2) \frac{\{3\Omega^2 - j(j+1)\}\{3/4 - j(j+1)\}}{(2j-1)j(j+1)(2j+3)}$$
$$\times \left(N + \frac{3}{2}\right) \frac{\hbar}{m\omega_0},\qquad(6)$$

where Q_0^c is a quadrupole moment of the core, v_i^2 is an occupation probability of the ith orbital, and $u_i^2 = 1 - v_i^2$; $\hbar/(m\omega_0) = 1.02A^{1/3}$; N, j, and Ω are the oscillator quantum
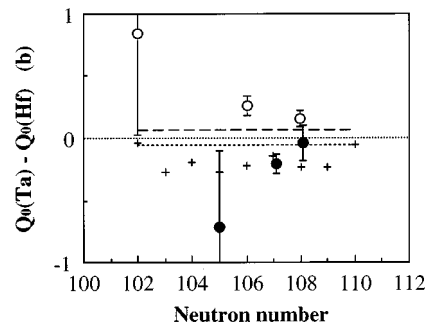

FIG. 6. Deviations of intrinsic quadrupole moments of Ta from those of the core nuclei Hf. Open circles are for the ground states and closed ones for the isomeric states. $+$ symbols are estimated values from theoretical calculations given in [16]. Dashed and dotted lines indicate the calculated values using Eq. (6) for the $7/2^+[404]_\pi$ and the $9/2^-[514]_\pi$ states, respectively.

number, the total angular momentum, and the projection on the symmetry axis, respectively, for the single particle. So we have the intrinsic quadrupole moments for both the $7/2^+[404]_\pi$ and the $9/2^-[514]_\pi$ states: $Q_0^{7/2} = Q_0^c - 0.211(u_{7/2}^2 - v_{7/2}^2)$ and $Q_0^{9/2} = Q_0^c - 0.131(u_{9/2}^2 - v_{9/2}^2)$. The parameters v_i^2 and u_i^2 can be calculated using the equation

$$v_i^2 = \frac{1}{2}\left(1 - \frac{\epsilon_i - \lambda}{\sqrt{(\epsilon_i - \lambda)^2 + \Delta^2}}\right), \qquad (7)$$

where ϵ_i is a single-particle energy, λ the Fermi energy, and Δ the pairing gap. The difference of single-particle energies between the two states is $\epsilon_{9/2} - \epsilon_{7/2} \sim 600$ keV at a nuclear deformation of $\beta \sim 0.28$ that is obtained from the intrinsic quadrupole moment of ^{181}Ta in the limit of a well-deformed rigid rotor (see Table II). The Fermi surface for protons is between the two single-particle states and Δ is about 1 MeV in this region according to [17]. The changes are thus estimated to be $Q_0^{7/2} - Q_0^c = +0.06$ b and $Q_0^{9/2} - Q_0^c = -0.04$ b (see Fig. 6). These values are so small, but the signs have a definite meaning compared to [16].

The present calculation explains well the signs of both changes found experimentally. It is, however, unable to reproduce the experimental values quantitatively. Discrepancy between the calculations and the experimental values should be mainly due to the core polarization effect that is not taken into account in the present calculation. The core polarization effect relates to the excitation energy of the β-vibrational state in the core nucleus. It is expected that the core polarization effect becomes smaller with increasing neutron num-ber because the excitation energy of the β-vibrational band-head in Hf nuclei becomes higher with increasing neutron number [19,20]. This expectation matches the experimental trend shown in Fig. 6. It is, however, difficult to calculate the contribution of the core polarization effect using presently available theories.

V. CONCLUSION

By means of high-resolution laser spectroscopy, we have determined the magnetic dipole and electric quadrupole moments of the ground state of ^{179}Ta for the first time. The magnetic moment of ^{179}Ta is in good agreement with the systematics. It is also concluded that the quadrupole moments of the $7/2^+[404]_\pi$ ground states are getting larger than those of the core nuclei Hf with decreasing neutron number, and by contrast those of the $9/2^-[514]_\pi$ isomeric states are getting smaller. Further measurements of μ_I and Q_s for neutron-deficient Ta isotopes would be desirable to understand the details of the nuclear structure in this mass region where high-spin isomers exist.

[1] E. W. Otten, in *Treatise on Heavy-Ion Science*, edited by D. A. Bromly (Plenum, New York, 1989), Vol. 8, p. 517.

[2] J. Rink, B. Gorski, W. Kälber, G. Meisel, H.-J. Mielke, H. Rebel, and M. Schubert, Z. Phys. A **342**, 487 (1992).

[3] N. Boos, F. Le Blanc, M. Krieg, J. Pinard, G. Huber, M. D. Lunney, D. Le Du, R. Meunier, M. Hussonnois, O. Constantinescu, J. B. Kim, Ch. Briancon, J. E. Crawford, H. T. Duong, Y. P. Gangrski, T. Kühl, B. N. Markov, Yu. Ts. Oganessian, P. Quentin, B. Roussière, and J. Sauvage, Phys. Rev. Lett. **72**, 2689 (1994).

[4] J. Schecker, A. Berger, J. Das, S. Dutta, G. Gwinner, C. H. Holbrow, T. Kühl, T. Lauritsen, G. D. Sprouse, and F. Xu, Phys. Rev. A **46**, 3730 (1992).

[5] A. Ya. Anastasov, Yu. P. Gangrskii, B. N. Markov, S. G. Zemlyanoi, B. K. Kul'dzhanov, and K. P. Marinova, Sov. Phys. JETP **78**, 132 (1994).

[6] P. Manfrass, W. Andrejtscheff, P. Kemnitz, E. Will, and G. Winter, Nucl. Phys. A **226**, 157 (1974).

[7] D. Barnéous, S. André, and C. Foin, Nucl. Phys. A **379**, 205 (1982).

[8] E. Warde, R. Seltz, D. Magnac, and H. L. Sharma, Phys. Rev. C **25**, 2353 (1982).

[9] M. Wakasugi, W. G. Jin, T. T. Inamura, T. Murayama, T. Wakui, T. Kashiwabara, H. Katsuragawa, T. Ariga, T. Ishizuka, M. Koizumi, and I. Sugai, Rev. Sci. Instrum. **64**, 3487 (1993).

[10] M. Wakasugi, W. G. Jin, T. T. Inamura, T. Murayama, T. Wakui, H. Katsuragawa, T. Ariga, T. Ishizuka, and I. Sugai, Phys. Rev. A **50**, 4639 (1994).

[11] W. G. Jin, M. Wakasugi, T. T. Inamura, T. Murayama, T. Wakui, H. Katsuragawa, T. Ariga, T. Ishizuka, and I. Sugai, Phys. Rev. A **50**, 1920 (1994).

[12] M. Blann and H. K. Vonach, Phys. Rev. C **28**, 1475 (1983).

[13] H. Kopfermann, *Nuclear Moments* (Academic Press, New York, 1958).

[14] P. Raghavan, Atom. Data Nucl. Data Tables **42**, 189 (1989).

[15] A. Bohr and V. F. Weisskopf, Phys. Rev. **77**, 94 (1950).

[16] C. Ekström, H. Rubinsztein, and P. Möller, Phys. Scr. **14**, 199 (1976).

[17] A. Bohr and B. R. Mottelson, *Nuclear Structure* (W. A. Benjamin, Reading, 1975), Vol. 2.

[18] S. Raman, C. H. Malarkey, W. T. Milner, C. W. Nestor, Jr., and P. H. Stelson, Atom. Data Nucl. Data Tables **36**, 1 (1987).

[19] C. M. Lederer and V. S. Shirley, *Table of Isotopes*, 7th ed. (John Wiley & Sons, Inc., New York, 1978).

[20] M. Sakai, Atom. Data Nucl. Data Tables **31**, 399 (1984).